



Cite this: DOI: 10.1039/c8nj01631c

# Water switched aggregation/disaggregation strategies of a coumarin–naphthalene conjugated sensor and its selectivity towards $\text{Cu}^{2+}$ and $\text{Ag}^+$ ions along with cell imaging studies on human osteosarcoma cells (U-2 OS)†

 Ashish Kumar,<sup>a</sup> Surajit Mondal,<sup>a</sup> Kumari Somlata Kayshap,<sup>a</sup> Sumit Kumar Hira,<sup>b</sup> Partha Pratim Manna,<sup>c</sup> Wim Dehaen<sup>d</sup> and Swapan Dey \*<sup>a</sup>
Received 4th April 2018,  
Accepted 18th May 2018

DOI: 10.1039/c8nj01631c

rsc.li/njc

A simple coumarin–naphthalene conjugated chemosensor (**R1**) exhibited an excellent AIE effect in methanol/water (50/50, v/v) with a perfect rectangular shape of aggregation, which was confirmed by SEM analysis. **R1** could recognise  $\text{Cu}^{2+}$  ions functioning as a selective chemosensor and identify  $\text{Ag}^+$  in a chemodosimeter approach. The biocompatibility of **R1** and bio-sensing of  $\text{Cu}^{2+}/\text{Ag}^+$  ions were also evaluated in human osteosarcoma cells (U-2 OS). A single crystal X-ray analysis confirmed the structure as well as the hydrogen bonding interaction for the dimerization of the compound.

## Introduction

Aggregation induced emission (AIE) is now widely studied, because of its promising applications in organic light-emitting diodes,<sup>1</sup> chemosensors,<sup>2</sup> fluorescent bioprobes,<sup>3</sup> mechanochromic materials<sup>4</sup> etc. In 2001, Tang's group discovered the novel phenomenon of aggregation-induced emission (AIE) which attracted attention because it offers a good opportunity to solve many key problems.<sup>4–6</sup> Molecules having hexaphenylsilole (HPS),<sup>7</sup> or tetraphenylethylene (TPE)<sup>8,9</sup> moieties were reported as very good AIE chemosensors. In addition to this, some conjugated groups like polyarylated ethenes,<sup>10</sup> butadienes,<sup>11</sup> pyrans,<sup>12</sup> and fulvenes<sup>13</sup> were also found to have substantial AIE effects in different solvents. AIE based chemosensors have also been extensively used in supramolecular chemistry, medicinal chemistry and biological chemistry.<sup>14</sup> Beside these, AIE chemosensors are also

highly in demand for selective sensing of heavy and noxious metal ions.<sup>15</sup> Coumarin and naphthalene have both been used as fluorophores in different sensors reported earlier.<sup>16–18</sup> Fluorescent sensors have several advantages over other methods due to their specificity, sensitivity, and very fast response towards complexation.<sup>19,20</sup> Small molecules based on fluorescence sensing probes are generally more attractive for metal ion detection in relation to AIE and bioimaging.<sup>21</sup> Previously, a metal ion like  $\text{Cu}^{2+}$  was used as a fluorescence quencher through an energy and electron transfer process.<sup>18,22</sup> A high concentration of  $\text{Ag}^+$  ions also creates adverse health effects and brain damage.<sup>23a,b</sup> These adverse effects of  $\text{Cu}^{2+}$  and  $\text{Ag}^+$  ions create a need to develop a highly selective and sensitive chemosensor to serve both environmental and human health purposes.<sup>23c–g</sup>

Thus, a new compound (**R1**) was developed in our laboratory which showed AIE in a certain proportion of water present in methanol. The compound is also effective to recognize  $\text{Cu}^{2+}$  and  $\text{Ag}^+$  using a higher wavelength output. Possible utilization of **R1** as an intracellular sensor of  $\text{Cu}^{2+}$  and  $\text{Ag}^+$  ions was also evaluated by fluorescence microscopy.

The coumarin–naphthalene conjugated chemosensor (**R1**) was synthesized through a simple reaction of 1-isothiocyanato-naphthalene and 3-amino-7-diethylaminocoumarin, resulting in a thiourea linkage between the two moieties (Scheme 1). The compound 3-amino-7-diethylaminocoumarin (**4**) was prepared following previous reports.<sup>24</sup> All compounds were characterized by FTIR, <sup>1</sup>H-NMR, <sup>13</sup>C-NMR, MS analysis and single crystal X-ray analysis and aggregation of **R1** was confirmed by SEM (Fig. 4).

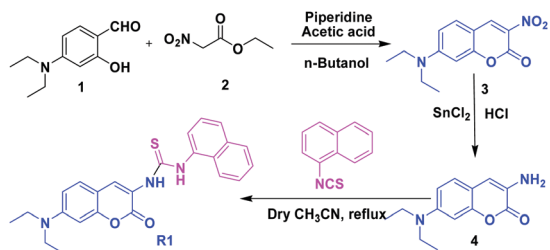
<sup>a</sup> Department of Applied Chemistry, Indian Institute of Technology (ISM), Dhanbad 826 004, Jharkhand, India. E-mail: swapan@iitism.ac.in; Fax: +91 326 2296563; Tel: +91 326 2235607

<sup>b</sup> Department of Zoology, The University of Burdwan, Burdwan, West Bengal 713104, India

<sup>c</sup> Department of Zoology, Institute of Science, Banaras Hindu University, Varanasi 221005, India

<sup>d</sup> Department of Chemistry, KU Leuven, Celestijnenlaan 200F, box: 3001, Belgium

† Electronic supplementary information (ESI) available: Experimental section, <sup>1</sup>H-NMR, <sup>13</sup>C-NMR, ESI-MS, FT-IR analysis, binding constant calculation, limit of detection, quantum yield calculation, biological applications, and single crystal X-ray structure of **R1**. CCDC 1552023. For the ESI and crystallographic data in CIF or other electronic format see DOI: 10.1039/c8nj01631c



Scheme 1 Synthetic route of R1.

## Experimental

All the chemicals were purchased from Sigma-Aldrich and Alfa-Aesar, and were used without additional purification. In the period of use, the solvents were distilled following usual procedure. Perchlorate salts were prepared in the laboratory, whereas, nitrate salts were purchased from Sigma-Aldrich. All reactions were done in dried glassware and the reaction mixtures were purified by silica gel column chromatography. For analysis,  $^1\text{H-NMR}$  and  $^{13}\text{C-NMR}$  spectra were recorded at 400 MHz and 100 MHz, respectively. For NMR analysis,  $\text{CDCl}_3$  solvent was used with TMS as a reference, and chemical shifts are assigned in  $\delta$  (ppm) units. Mass spectra (MS and HRSM) data were recorded in positive ion mode with an ESI source. UV-visible and fluorescence titrations were completed through a PerkinElmer Lambda 365 and LS 55, respectively, where the path length of the cuvette is 10 mm.

### General methods of photo-physical studies

Photo-physical (UV-vis and fluorescence) studies were carried out with a stock solution of R1 ( $c = 5.4 \times 10^{-6}$  M, at  $\text{pH} = 7.2 \pm 0.05$ ), which was prepared in  $\text{MeOH}:\text{H}_2\text{O}$  (9:1, v/v, at  $\text{pH} 7.2$ , HEPES buffer). Stock solutions of guest metal ions ( $10^{-4}$  M), such as  $\text{Al}^{3+}$ ,  $\text{K}^+$ ,  $\text{Cr}^{3+}$ ,  $\text{Mn}^{2+}$ ,  $\text{Fe}^{3+}$ ,  $\text{Fe}^{2+}$ ,  $\text{Co}^{2+}$ ,  $\text{Ni}^{2+}$ ,  $\text{Cu}^{2+}$ ,  $\text{Zn}^{2+}$ ,  $\text{Ag}^+$ ,  $\text{Cd}^{2+}$ ,  $\text{Ba}^{2+}$ ,  $\text{Hg}^{2+}$ ,  $\text{Pb}^{2+}$  and  $\text{Bi}^{3+}$  perchlorate and nitrate salts were prepared in 10 mL volumetric flasks. The UV-vis and fluorescence titration studies were performed taking a 2 mL solution of R1 in a cuvette and gradually increasing the concentration of metal ions.

### Synthesis of compound 3

4-(Diethylamino)salicylaldehyde (500 mg, 2.58 mmol) was dissolved in 1-butanol (15 mL), and ethyl nitroacetate (300  $\mu\text{L}$ , 2.83 mmol) was added to the solution. Piperidine (50  $\mu\text{L}$ ) and acetic acid (100  $\mu\text{L}$ ) were added to the reaction mixture in a catalytic amount. Then the reaction mixture was refluxed for 24 h with continuous stirring. After completion, it was removed from the oil bath and cooled at room temperature. A solid compound (3) was precipitated and isolated in pure form (yield 70%).<sup>24</sup>

### Synthesis of compound 4

Compound 3 (200 mg, 0.763 mmol) was taken in 5 mL concentrated hydrochloric acid, and 1.0 g (5.0 mmol) of tin chloride was added slowly to the reaction mixture over 15 minutes. The reaction mixture was stirred for 6 h at room temperature. The solution of the reaction mixture became transparent. An aqueous

solution of NaOH (4 N) was added to the reaction mixture until complete neutralization. The crude product was isolated by using 20 mL of ethylacetate. This process was repeated three times to ensure complete extraction. Anhydrous  $\text{MgSO}_4$  was added to the organic phase to completely remove water and it was concentrated under reduced pressure. Finally, coumarin amine (4) was obtained with a high yield (76%) and it was used for further reaction without purification.

### Synthesis of R1

3-Amino-7-diethylamino coumarin (4) (100 mg, 0.43 mmol) was dissolved in 20 mL of dry acetonitrile and 1-isothiocyanatophthalene (5) (80 mg, 0.43 mmol) was added into the coumarin solution. The reaction mixture was heated under reflux conditions for 24 h. The formation of the product was monitored through thin layer chromatography. After completion, distilled water (20 mL) was added and it was extracted three times with ethyl acetate (100 mL). Anhydrous  $\text{MgSO}_4$  was added to remove water and the desired compound (R1) was purified by column chromatography (silica gel) from the residue of evaporation under reduced pressure (product yield 45.0%, 80.0 mg). m.p.  $-162$  °C,  $^1\text{H-NMR}$  (400 MHz,  $\text{CDCl}_3$ ) of R1:  $\delta$  (ppm) 9.23 (s, 1H), 8.31 (s, 1H), 7.98 (d,  $J = 6.8$ , Hz, 1H), 7.89–7.85 (m, 3H), 7.53–7.49 (m, 4H), 7.25 (d,  $J = 8.8$  Hz, 1H) 7.18 (s, 1H), 6.53 (d,  $J = 8.8$  Hz, 1H), 6.36 (s, 1H) 3.31 (q,  $J = 7.2$  Hz, 4H), 1.11 (t,  $J = 7.2$  Hz, 6H).  $^{13}\text{C}$  NMR (125 MHz,  $\text{CDCl}_3$ ) of R1:  $\delta$  (ppm) 178.57, 160.09, 152.81, 149.69, 134.79, 131.45, 129.81, 129.39, 129.08, 128.67, 127.58, 127.37, 127.14, 125.87, 125.18, 122.17, 119.29, 109.60, 107.75, 97.32, 44.75, 12.46. ESI-MS (+): calculated  $\text{C}_{24}\text{H}_{23}\text{N}_3\text{O}_2\text{S}$ : 417.1511, found: 418.1583 [ $\text{M} + \text{H}^+$ , 50], 440.141 [ $\text{M} + \text{Na}$ , 100], 857.3092 [ $2\text{M} + \text{Na}$ , 98].

### Reagents & cells

The culture medium used throughout the study was RPMI-1640 supplemented with penicillin (100 U  $\text{mL}^{-1}$ ) and streptomycin (100  $\mu\text{g mL}^{-1}$ ) (Cell clone, Genetix, India) and 10% fetal bovine serum (Cell clone, Genetix, India). Henceforth, this combination was considered as complete medium. Other general and fine chemicals were procured from SIGMA, USA, unless otherwise stated. Human bone osteosarcoma cells U-2 OS (ATCC HTB-96<sup>TM</sup>) were cultured in complete medium. Human peripheral blood mononuclear cells (PBMCs) were separated from whole blood using the Ficoll Hypaque technique as described earlier.<sup>25</sup> Monocytes and lymphocytes were isolated from PBMC as described by us before.<sup>26</sup> The cells were washed in phosphate buffer saline (PBS) twice, and suspended in complete medium before use.

### Cellular imaging study

In order to investigate the possible application of the coumarin based chemosensor (R1), we have explored the suitability of the compound as a chemosensor in bio-imaging. U-2 OS cells were incubated in the presence or absence of varying concentrations ( $0$ ,  $1 \times 10^{-6}$ ,  $1 \times 10^{-5}$  &  $1 \times 10^{-4}$  M) of  $\text{Cu}^{2+}$  and  $\text{Ag}^+$  ions for 4 hours (h) at 37 °C and 5%  $\text{CO}_2$  in culture medium. After washing with PBS ( $\times 3$ ), the remaining metal ions were removed

and the cells were incubated with **R1** ( $1 \times 10^{-5}$  M) for 1 hour at room temperature. The cells were washed with PBS ( $\times 2$ ) and fluorescence images of the cells were obtained using an EVOS<sup>®</sup> FL Cell Imaging System, Life Technologies, USA.

### Biocompatibility studies

The biocompatibility of the coumarin based chemosensor (**R1**) or the **R1:Cu<sup>2+</sup>** and **R1:Ag<sup>+</sup>** complex was assessed by an MTT assay for the proliferation of U-2 OS cells as described earlier.<sup>27</sup> The lytic activity of the above compounds against U-2 OS cells was measured by a non-radioactive cytotoxicity assay using the CytoTox 96 Non-Radioactive Cytotoxicity assay kit (Promega, USA). U-2 OS cells ( $5 \times 10^3$ ) were added to a 96-well tissue culture dish and exposed to serial concentrations (10, 25, 50, and 100  $\mu$ M) of free **R1** or **R1**-loaded ions and incubated for 18 h at 37 °C, 5% CO<sub>2</sub>. Percent-specific lysis was determined using the formula described earlier.<sup>27</sup>

### Hemocompatibility studies

The effect of the coumarin based chemosensor (**R1**) on the viability of human monocytes and lymphocytes was evaluated by a colorimetric XTT (sodium 3-[1-(phenylaminocarbonyl)-3,4-tetrazolium]-bis(4-methoxy-6-nitro)benzene sulfonic acid hydrate) assay (Roche Molecular Biochemicals, Indianapolis, IN).<sup>3</sup> Human monocytes or lymphocytes ( $5 \times 10^3$  cells per well) were plated in a 96-well culture dish and exposed to serial concentrations (10, 25, 50, and 100  $\mu$ M) of the compounds and incubated at 37 °C, 5% CO<sub>2</sub>, for 18 h. OD was measured at 450 nm using a Synergy HT Multi-Mode Microplate Reader, BioTek, USA. The data were presented as the percentage of viable cells calculated from the formula reported earlier.<sup>28</sup>

A hemolysis assay was performed as previously described by us.<sup>3</sup> In brief, normal human RBCs were treated with increasing concentrations of **R1** for 4 h at 37 °C. The percentage of haemolysis was determined by using the formula as described by us before.<sup>27</sup>

### Statistical analysis

The mean  $\pm$  SD was calculated for each experimental group. “*n*” represents the number of times the experiment was performed. Differences between the groups were analyzed by unpaired Student's *t*-test and one- or two-way analysis of variance (ANOVA) depending on the requirement.

## Results and discussion

The photo-physical experiments of **R1** ( $c = 5.4 \times 10^{-6}$  M) were carried out using UV-vis and fluorescence techniques in MeOH:H<sub>2</sub>O (9:1, v/v, at pH-7.2, HEPES buffer) with various nitrate/perchlorate salts of metal ions, such as Al<sup>3+</sup>, K<sup>+</sup>, Cr<sup>3+</sup>, Mn<sup>2+</sup>, Fe<sup>3+</sup>, Fe<sup>2+</sup>, Co<sup>2+</sup>, Ni<sup>2+</sup>, Cu<sup>2+</sup>, Zn<sup>2+</sup>, Ag<sup>+</sup>, Cd<sup>2+</sup>, Ba<sup>2+</sup>, Hg<sup>2+</sup>, Pb<sup>2+</sup>, and Bi<sup>3+</sup>. Amongst the metal ions tested, only Cu<sup>2+</sup> and Ag<sup>+</sup> ions cause a change in the fluorescence intensity, which was also explained using a bar diagram (ESI,<sup>†</sup> Fig. S8).

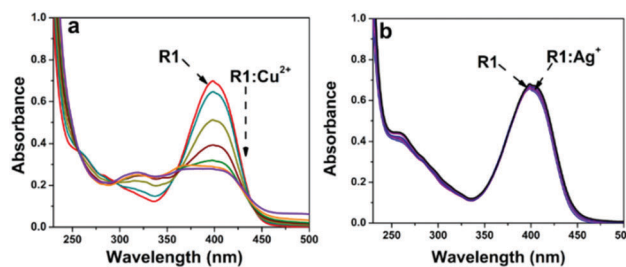
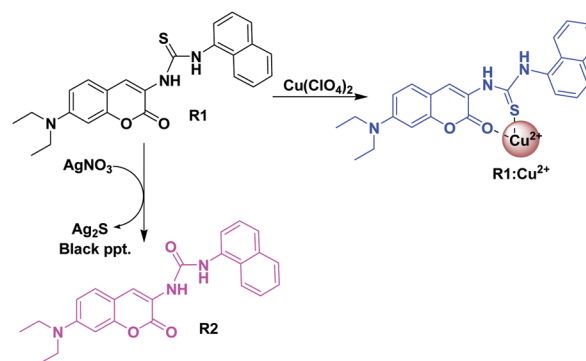


Fig. 1 UV-vis titration of **R1** in MeOH:H<sub>2</sub>O (9:1, v/v, at pH-7.2, HEPES buffer) (a) with continuous addition of Cu<sup>2+</sup> ions and (b) with continuous addition of Ag<sup>+</sup> ions.

The UV-vis absorption spectrum of **R1** contains a peak at  $\lambda_{\text{max}}$  400 nm and titration was carried out with Cu<sup>2+</sup> and Ag<sup>+</sup> ions, separately. The observed peak intensity was continuously decreased in the presence of Cu<sup>2+</sup> and two isosbestic points were generated at  $\lambda_{\text{max}}$  360 nm and  $\lambda_{\text{max}}$  437 nm (Fig. 1a), but in the presence of Ag<sup>+</sup> ions, no changes were observed in the absorption spectrum of **R1** (Fig. 1b).

**R1** itself shows weak fluorescence properties, and the fluorescence intensity was enhanced continuously upon the addition of Cu<sup>2+</sup> ions. When it was excited at  $\lambda_{\text{ex}}$  400 nm, the emission spectra at  $\lambda_{\text{em}}$  480 nm were recorded, accordingly. Moreover, the fluorescence intensity of **R1** has been quenched and a new compound **R2** was formed (Scheme 2), upon addition of Ag<sup>+</sup> ions (Fig. 2). In the presence of Ag<sup>+</sup> ions, the fluorescence intensity was quenched without the formation of a new emission band, which resulted in quenching of the fluorescence intensity through an energy-transfer (ET) process.<sup>28b,c</sup> According to Hard and Soft Acid and Base (HSAB) theory,<sup>29</sup> the S-atom behaves as a soft base, and it has a more polarized lone pair of electrons, which can easily form a complex with soft acids (Ag<sup>+</sup> ions).<sup>30a-d</sup> Therefore, Ag<sup>+</sup> ions formed a stable complex with the S-atom of thiourea in order to convert **R2**. Consequently, when the S-atom was replaced by the O-atom, the fluorescence emission intensity was low because the O-atom worked as a fluorescence quencher.<sup>30e,f</sup>

Most of the metal ions (up to 10.0 equivalents) did not cause significant changes to the peak shifting of **R1**. Besides these, photo-physical studies of **R1** ( $c = 5.0 \times 10^{-6}$  M) have also been carried out in a mixture of solvents by changing the percentage



Scheme 2 Probable mode of complexation of **R1** with Cu<sup>2+</sup> and Ag<sup>+</sup> and the formation of **R2** in the presence of AgNO<sub>3</sub>.

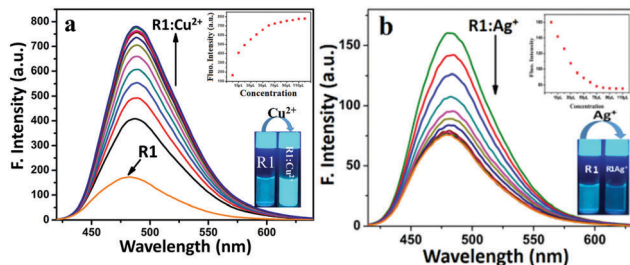


Fig. 2 Fluorescence titration spectra of **R1** ( $c = 5.4 \times 10^{-6}$  M) in MeOH:H<sub>2</sub>O (9:1, v/v, pH-7.2, HEPES buffer) (a) with Cu<sup>2+</sup> ions up to 3.0 equiv. and (b) with Ag<sup>+</sup> ions up to 3.0 equiv. (Inset: Fluorescence change).

of water in the methanol–water mixture. The fluorescence intensity of **R1** was changed with different fractions of water in methanol (Fig. 4a). **R1** showed a weak fluorescence in pure methanol, but the addition of water in methanol continuously increased the fluorescence intensity until the MeOH/H<sub>2</sub>O ratio became 1:1. After that the fluorescence intensity was quenched sharply with an increase in the percentage of water (up to 90%) in methanol (Fig. 4a). The enhancement in fluorescence intensity has been explained as a result of the morphological changes like the aggregation induced emission (AIE) of the chemosensor **R1** varying the percentage of water in methanol. Above, the course of disaggregation quenched the fluorescence intensity through a disaggregation-caused quenching (DCQ) mechanism with the help of SEM analysis.

The quantum yield ( $\phi$ ) and corresponding  $\lambda_{\max}$  of **R1** itself in different solvents and its complex with Cu<sup>2+</sup> and Ag<sup>+</sup> were calculated in methanol and are shown in Fig. 3. The binding constants ( $K_a$ ) of **R1**:Cu<sup>2+</sup> and **R1**:Ag<sup>+</sup> were found to be  $1.9 \times 10^5$  M<sup>-1</sup> and  $1.5 \times 10^5$  M<sup>-1</sup> respectively.<sup>31</sup> The detection limits of **R1** were recorded as  $8.1 \times 10^{-9}$  M and  $44.0 \times 10^{-9}$  M for Cu<sup>2+</sup> and Ag<sup>+</sup> ions, respectively.<sup>32</sup>

The SEM images as shown in Fig. 4b(i–iv) depicted that, in pure methanol (10-0), the size of **R1** was not predictable. But, in the case of the 50% water in methanol mixture, **R1** was observed to have an aggregated morphology with rectangular shape and this is shown in a magnified view in Fig. 4b(iv). Furthermore, the aggregation was destroyed in a 90% water–methanol mixture and no prominent image was obtained [Fig. 4b(ii)]. The aggregated surface morphology in 50% water–methanol caused an enhancement in the fluorescence intensity, which was gradually quenched on further addition of water.

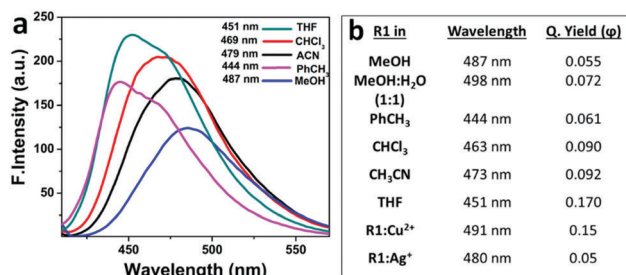


Fig. 3 **R1** in different organic solvents; (a) fluorescence spectra and (b) wavelength ( $\lambda_{\max}$ ) and quantum yield ( $\phi$ ).

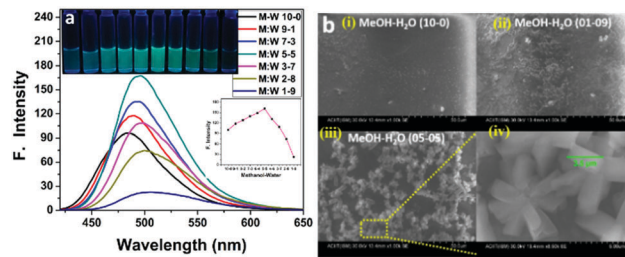


Fig. 4 (a) Effect of fluorescence intensity and (b) SEM images of different proportions of H<sub>2</sub>O in CH<sub>3</sub>OH.

Fortunately, a single crystal of **R1** was grown by slow evaporation of 20% methanol in chloroform. Each unit cell consists of two molecules ( $Z = 2$ ) with a *P1* space group and triclinic system. The solid-state structure of compound **R1** is quite interesting having short contacts and hydrogen-bonding interactions. The molecule took part in the complementary dimerization of S···H–N and N–H···S with two hydrogen bonding interactions (Fig. 5). Short contact interactions are important for propagating the chain in a supramolecular array. The stacking interaction between the two coumarin rings was also found at a distance of 3.47 Å, which helped in aggregation of the molecules in water.

According to the <sup>1</sup>H-NMR spectra of **R1**, two NH protons of **R1** were observed at  $\delta$  9.24 (1H, s) and  $\delta$  6.36 (1H, s) ppm and the coumarin proton at C4 appeared at  $\delta$  8.31 ppm (1H, s). After the addition of Cu(ClO<sub>4</sub>)<sub>2</sub>, the three mentioned protons of **R1** were shifted to  $\delta$  9.97 ppm, 6.58 ppm (down field) and  $\delta$  8.28 ppm (up field), respectively. AgNO<sub>3</sub> was highly reactive towards **R1** which caused the replacement of the S-atom of thiourea into a urea linkage (**R2**, Scheme 2). This observation was clearly supported by mass spectroscopy as peaks appeared at 402.1897 (**R2** + H<sup>+</sup>) and 424.1626 (**R2** + Na<sup>+</sup>). As a result, when AgNO<sub>3</sub> was reacted with chemosensor **R1**, a black precipitate of Ag<sub>2</sub>S was isolated and the fluorescence intensity was quenched (Fig. 2b).

Quantum chemical calculations were carried out using the Gaussian 09 program with the Gauss-View 5.0 visualization

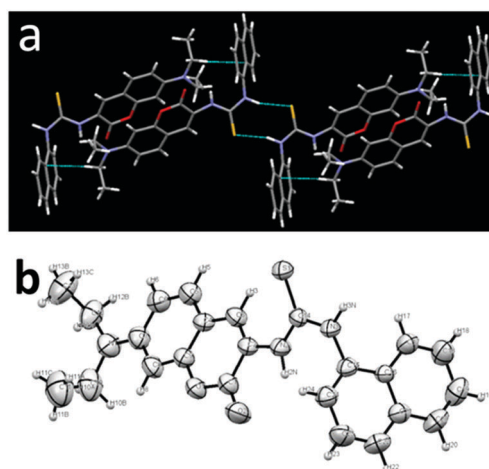


Fig. 5 Single crystal X-ray structure of **R1**: (a) short contact and H-bonding interactions and (b) ORTEP diagram of **R1**.

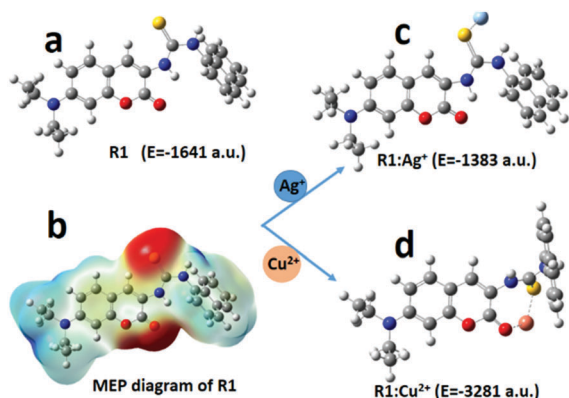


Fig. 6 (a) Optimized structure of **R1** using the DFT/B3LYP/6-311G method. (b) MEP diagram of **R1**. (c) Optimized structure of **R1:Ag<sup>+</sup>** using the Lan2LMB method. (d) Optimized structure of **R1:Cu<sup>2+</sup>** using the B3LYP/6-311G method.

program.<sup>33</sup> The density functional theory (DFT) method was applied for the optimization of the structures of **R1**, **R1:Ag<sup>+</sup>** and **R1:Cu<sup>2+</sup>** using a different basis set. The basis set B3LYP/6-311G was applied for **R1** and **R1:Cu<sup>2+</sup>** and Lan2LMB for **R1:Ag<sup>+</sup>**. The Molecular Electrostatic Potential (MEP) diagram (Fig. 6b) of **R1** is shown in red and blue colour, where red colour indicates an electron rich region and blue colour is for any electron deficient region. The red colour is located above the electronegative S atom and two O atoms of coumarin. The total energy of **R1** ( $E = -1641$  a.u.) was higher compared to **R1:Cu<sup>2+</sup>** ( $-3218$  a.u.) and lower compared to **R1:Ag<sup>+</sup>** ( $-1383$  a.u.), so it clearly indicated that **R1** was less stable than **R1:Cu<sup>2+</sup>** and more stable than **R1:Ag<sup>+</sup>** (Fig. 6).

We further investigated intracellular fluorescence for visualization of **R1** with **Cu<sup>2+</sup>** and **Ag<sup>+</sup>** ions in live cells. Human osteosarcoma cells U-2 OS were first incubated with various concentrations ( $0$ ,  $1 \times 10^{-6}$  M,  $1 \times 10^{-5}$  M and  $1 \times 10^{-4}$  M) of  $\text{Cu}(\text{ClO}_4)_2$  (Fig. 7) for 4.0 h followed by treatment with  $1 \times 10^{-5}$  M **R1** for 30 minutes before imaging.

Very negligible fluorescence was observed in the cells (Fig. 7E and I) that were exposed to only **R1**, while strong fluorescence

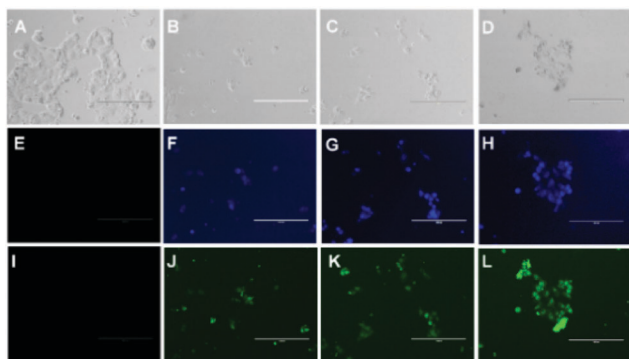


Fig. 7 Representative fluorescence images of U-2 OS cells exposed to various concentrations of  $\text{Cu}(\text{ClO}_4)_2$  in **R1** ( $1 \times 10^{-5}$  M). (A, E and I) **R1** only, (B, F and J) **R1** with  $1 \times 10^{-6}$  M **Cu<sup>2+</sup>**, (C, G and K) **R1** with  $1 \times 10^{-5}$  M **Cu<sup>2+</sup>**, and (D, H and L) **R1** with  $1 \times 10^{-4}$  M **Cu<sup>2+</sup>** for 4 h followed by **R1**.

was observed in the cells [Fig. 7F–H and J–L] with different concentrations of  $\text{Cu}(\text{ClO}_4)_2$ . The blue and green fluorescence were observed when their respective filters were used. The cell (U-2 OS) proliferation and direct cytotoxicity of **R1** as well as its complexes were investigated (ESI,† Fig. S14) along with hemolysis and viability (ESI,† Fig. S15), which concluded that **R1** was safe and non-toxic to live cells.

## Conclusions

In conclusion, a simple chemosensor (**R1**) was reported which was built up with coumarin–thiourea–naphthalene moieties. The sensor exhibited an important role in sensing, bio-imaging, and solvent induced aggregation/disaggregation. Aggregation induced emission (AIE) with the increase of water content up to 50% in methanol and disaggregation-caused quenching (DCQ) on raising the percentage of water in methanol above 50% were observed. AIE and DCQ both were confirmed by fluorescence spectroscopy and SEM imaging. Besides these, **R1** is also a very good sensor for **Cu<sup>2+</sup>** and **Ag<sup>+</sup>** selectively in methanol at  $\text{pH} = 7.2 \pm 0.05$ , in HEPES buffer solution. In addition to that  $\text{AgNO}_3$  reacted with **R1** replacing the S-atom of the thiourea linkage to convert it to a urea linkage (**R2**). All of this evidence was confirmed by  $^1\text{H-NMR}$  and mass analysis. The limit of detection and binding constant between host and guest were calculated using the usual methods. It was shown that **R1** and its metallated derivatives were safe and non-toxic to a wide range of cells including WBCs and RBCs, and did not hinder cellular growth, indicating its suitability as a biosensor.

## Conflicts of interest

There are no conflicts to declare.

## Acknowledgements

SD acknowledges SERB-DST, Govt. of India for the financial assistance (project no. EMR/2016/002183) and AREAS+ (under Erasmus Mundus) for providing a postdoctoral fellowship. AK, SM and KSK are thankful to IIT (ISM), Dhanbad for providing a research fellowship.

## Notes and references

- Z. Zhao, J. W. Y. Lam and B. Z. Tang, *J. Mater. Chem.*, 2012, **22**, 23726–23740.
- M. Wang, G. Zhang, D. Zhang, D. Zhu and B. Z. Tang, *J. Mater. Chem.*, 2010, **20**, 1858–1867.
- W. Qin, D. Ding, J. Liu, W. Z. Yuan, Y. Hu, B. Liu and B. Z. Tang, *Adv. Funct. Mater.*, 2012, **22**, 771–779.
- J. Wang, J. Mei, R. Hu, J. Z. Sun, A. Qin and B. Z. Tang, *J. Am. Chem. Soc.*, 2012, **134**, 9956–9966.
- Y. Hong, J. W. Y. Lam and B. Z. Tang, *Chem. Soc. Rev.*, 2011, **40**, 5361–5388.

- 6 J. Shi, N. Chang, C. Li, J. Mei, C. Deng, X. Luo, Z. Liu, Z. Bo, Y. Q. Dong and B. Z. Tang, *Chem. Commun.*, 2012, **48**, 10675–10677.
- 7 J. Chen, C. C. W. Law, J. W. Y. Lam, Y. Dong, S. M. F. Lo, I. D. Williams, D. Zhu and B. Z. Tang, *Chem. Mater.*, 2003, **15**, 1535–1546.
- 8 Y. Hong, J. W. Y. Lam and B. Z. Tang, *Chem. Commun.*, 2009, 4332–4353.
- 9 X. Liu and G. Liang, *Chem. Commun.*, 2017, **53**, 1037–1040.
- 10 J. Chen, B. Xu, X. Ouyang, B. Z. Tang and Y. Cao, *J. Phys. Chem. A*, 2004, **108**, 7522–7526.
- 11 H. Tong, Y. Hong, Y. Dong, Y. Ren, M. Häußler, J. W. Y. Lam, K. S. Wong and B. Z. Tang, *J. Phys. Chem. B*, 2007, **111**, 2000–2007.
- 12 H. Tong, Y. Dong, Y. Hong, M. Häußler, J. W. Y. Lam, H. H. Y. Sung, X. Yu, J. Sun, I. D. Williams, H. S. Kwok and B. Z. Tang, *J. Phys. Chem. C*, 2007, **111**, 2287–2294.
- 13 Q. Zeng, Z. Li, Y. Dong, C. A. Di, A. Qin, Y. Hong, L. Ji, Z. Zhu, C. K. W. Jim, G. Yu, Q. Li, Z. Li, Y. Liu, J. Qin and B. Z. Tang, *Chem. Commun.*, 2007, 70–72.
- 14 H.-C. Hung, C.-W. Cheng, Y.-Y. Wang, Y.-J. Chen and W.-S. Chung, *Eur. J. Org. Chem.*, 2009, 6360–6366.
- 15 X. Qi, E. J. Jun, L. Xu, S.-J. Kim, J. S. Joong Hong, Y. J. Yoon and J. Yoon, *J. Org. Chem.*, 2006, **71**, 2881–2884.
- 16 D. Maity and T. Govindaraju, *Inorg. Chem.*, 2010, **49**, 7229–7231.
- 17 D. Maity and T. Govindaraju, *Inorg. Chem.*, 2011, **50**, 11282–11284.
- 18 J.-S. Wu, W.-M. Liu, X.-Q. Zhuang, F. Wang, P.-F. Wang, S.-L. Tao, X.-H. Zhang, S.-K. Wu and S.-T. Lee, *Org. Lett.*, 2007, **9**, 33–36.
- 19 H. S. Jung, P. S. Kwon, J. W. Lee, J. I. Kim, C. S. Hong, J. W. Kim, S. Yan, J. Y. Lee, J. H. Lee, T. Joo and J. S. Kim, *J. Am. Chem. Soc.*, 2009, **131**, 2008–2012.
- 20 (a) A. Kumar, C. Kumari, D. Sain, S. K. Hira, P. P. Manna and S. Dey, *ChemistrySelect*, 2017, **2**, 2969–2974; (b) S. Goswami, A. Manna, S. Paul, A. K. Maity, P. Saha, C. K. Quah and H.-K. Fun, *RSC Adv.*, 2014, **4**, 34572–34576; (c) S. Goswami, S. Paul and A. Manna, *RSC Adv.*, 2013, **3**, 25079–25085; (d) S. Paul, A. Manna and S. Goswami, *Dalton Trans.*, 2015, **44**, 11805–11810.
- 21 Q. Wang, Z. Li, D.-D. Tao, Q. Zhang, P. Zhang, D.-P. Guo and Y.-B. Jiang, *Chem. Commun.*, 2016, **52**, 12929–12939.
- 22 A. W. Varnes, R. B. Dodson and E. L. Wehry, *J. Am. Chem. Soc.*, 1972, **94**, 946–950.
- 23 (a) K. S. Park, J. Y. Lee and H. G. Park, *Chem. Commun.*, 2012, **48**, 4549–4551; (b) K. Ghosh, S. Panja and T. Sarkar, *Supramol. Chem.*, 2015, **23**, 490–500; (c) K. Ghosh and T. Sarkar, *Supramol. Chem.*, 2011, **23**, 435–440; (d) K. Ghosh, T. Sarkar and D. Tarafdar, *Supramol. Chem.*, 2012, **24**, 197–203; (e) K. Ghosh, T. Sarkar, A. Samadder and A. R. Khuda-Bukhshb, *New J. Chem.*, 2012, **36**, 2121–2127; (f) Z. Xu, J. Yoon and D. R. Spring, *Chem. Commun.*, 2010, **46**, 2563–2565; (g) H. Xu, X. Wang, C. Zhang, Y. Wu and Z. Liu, *Inorg. Chem. Commun.*, 2013, **34**, 8–11.
- 24 C. Y. Ang, S. Y. Tan, S. Wu, Q. Qu, M. F. E. Wong, Z. Luo, P.-Z. Li, S. Tamil Selvan and Y. Zhao, *J. Mater. Chem. C*, 2016, **4**, 2761–2774.
- 25 S. Kumar Hira, I. Mondal, D. Bhattacharya and P. P. Manna, *Exp. Cell Res.*, 2014, **327**, 192–208.
- 26 S. K. Hira, I. Mondal, D. Bhattacharya, K. K. Gupta and P. P. Manna, *Int. J. Biochem. Cell Biol.*, 2015, **67**, 1–13.
- 27 S. K. Hira, K. Ramesh, U. Gupta, K. Mitra, N. Misra, B. Ray and P. P. Manna, *ACS Appl. Mater. Interfaces*, 2015, **7**, 20021–20033.
- 28 (a) S. K. Hira, A. K. Mishra, B. Ray and P. P. Manna, *PLoS One*, 2014, **9**, 94309; (b) X. Yong, W. Wan, M. Su, W. You, X. Lu, Y. Yan, J. Qu, R. Liu and T. Masuda, *Polym. Chem.*, 2013, **4**, 4126–4133; (c) W. Zeng, X. Yong, X. Yang, Y. Yan, X. Lu, J. Qu and R. Liu, *Macromol. Chem. Phys.*, 2014, **215**, 1370–1377.
- 29 (a) R. G. Pearson, *J. Am. Chem. Soc.*, 1963, **85**, 3533–3539; (b) R. G. Pearson, *J. Chem. Educ.*, 1968, **45**, 581; (c) R. G. Pearson, *J. Chem. Educ.*, 1968, **45**, 643; (d) R. G. Pearson, *J. Chem. Educ.*, 1987, **64**, 561.
- 30 (a) G. A. Bowmaker, C. Pakawatchai, S. Saithong, B. W. Skelton and A. H. White, *Dalton Trans.*, 2009, 2588–2598; (b) G. A. Bowmaker, C. Pakawatchai, S. Saithong, B. W. Skelton and A. H. White, *Dalton Trans.*, 2010, **39**, 4391–4404; (c) F. B. Stocker, D. Britton and V. G. Young, *Inorg. Chem.*, 2000, **39**, 3479–3484; (d) A. A. Isab, S. Nawaz, M. Saleem, M. Altaf, M. Monim-ul-Mehboob, S. Ahmad and H. S. Evans, *Polyhedron*, 2010, **29**, 1251–1256; (e) J. R. Lakowicz, *Principles of Fluorescence Spectroscopy*, 2nd edn, 1999; (f) H. Kautsky, *Trans. Faraday Soc.*, 1939, **35**, 216–219.
- 31 C. Kumari, D. Sain, A. Kumar, H. P. Nayek, S. Debnath, P. Saha and S. Dey, *Sens. Actuators, B*, 2017, **243**, 1181–1190.
- 32 M. Shortreed, R. Kopelman, M. Kuhn and B. Hoyland, *Anal. Chem.*, 1996, **68**, 1414–1418.
- 33 A. Kumar, D. Sain, C. Kumari and S. Dey, *ChemistrySelect*, 2017, **2**, 1106–1110.